Hydrological and ecological changes in Western Europe between 3200 and 2000 years BP derived from lipid biomarker δD values in Lake Meerfelder Maar sediments

O. Rach[1,2*], S. Engels[3], A. Kahmen[4], A. Brauer[5], C. Martín-Puertas[5,6], B. van Geel[7], D. Sachse[1]

[1]GFZ German Research Centre for Geosciences, Section 5.1, Geomorphology, Organic Surface Geochemistry Lab, Telegrafenberg, D-14473 Potsdam, Germany

[2]Institute for Earth- and Environmental Science, University of Potsdam, Karl-Liebknecht-Strasse 24-25, 14476 Potsdam (Germany)

[3]Centre for Environmental Geochemistry, School of Geography, University of Nottingham, University Park, Nottingham (UK)

[4]Botany – Department of Environmental Sciences, University of Basel, Schönbeinstrasse 6, 4056 Basel (Switzerland)

[5]GFZ German Research Centre for Geosciences, Section 5.2 Climate Dynamics and Landscape Evolution, Telegrafenberg, 14473 Potsdam (Germany)

[6]Department of Geography, Royal Holloway, University of London, Egham, Surrey TW20 0EX, United Kingdom.

[7]Institute for Biodiversity and Ecosystem Dynamics, University of Amsterdam, Science Park 904, 1098 XH Amsterdam (Netherlands)

* Corresponding author's email address: oliver.rach@gfz-potsdam.de

Highlights

- We present a high-resolution late Holocene biomarker δD record from W Europe

- Terrestrial biomarker δD_{terr} records minor hydrological changes between 3.2-2.0 cal ka BP
- δD_{terr} data are in agreement with other paleoecological data
- We observe significant effects of aquatic lipid source changes on the δD_{aq} record
- Multiproxy approaches are essential to avoid hydrological misinterpretations

Keywords

Holocene; Climate dynamics; Paleoclimatology; Western Europe; Continental biomarkers; Organic geochemistry; Stable isotopes; Vegetation dynamics

Abstract

One of the most significant Late Holocene climate shifts occurred around 2800 years ago, when cooler and wetter climate conditions established in western Europe. This shift coincided with an abrupt change in regional atmospheric circulation between 2760 and 2560 cal years BP, which has been linked to a grand solar minimum with the same duration (the Homeric Minimum). We investigated the temporal sequence of hydroclimatic and vegetation changes across this interval of climatic change (Homeric climate oscillation) by using lipid biomarker stable hydrogen isotope ratios (δD values) and pollen assemblages from the annually-laminated sediment record from lake Meerfelder Maar (Germany).

Over the investigated interval (3200 to 2000 varve years BP), terrestrial lipid biomarker δD showed a gradual trend to more negative values, consistent with the western Europe long-term climate trend of the Late Holocene. At ca. 2640 varve years BP we identified a strong increase in aquatic plants and algal remains, indicating a rapid change in the aquatic ecosystem superimposed on this long-term trend. Interestingly, this aquatic ecosystem

change was accompanied by large changes in δD values of aquatic lipid biomarkers, such as nC_{21} and nC_{23} (by between 22-30‰). As these variations cannot solely be explained by hydroclimate changes, we suggest that these changes in the δD_{aq} value were influenced by changes in *n*-alkane source organisms. Our results illustrate that if ubiquitous aquatic lipid biomarkers are derived from a limited pool of organisms, changes in lake ecology can be a driving factor for variations on sedimentary lipid δD_{aq} values, which then could be easily misinterpreted in terms of hydroclimatic changes.

1. Introduction

Late Holocene climate was characterized by a gradual long-term cooling trend recognized globally (Marcott et al., 2013; Wanner et al., 2008), but also by superimposed short-term climatic variations occurring over the lifetime of a few generations and with strong impact on regional climate and society. For example, a relatively abrupt cooling and increased humidity 2800 years ago in the North Atlantic-European region (Swierczynski et al., 2013; Wirth et al., 2013) were interpreted from peat bog records in the Netherlands (van Geel et al., 1996; van Geel et al., 1999), glacial advances, and increased lake levels throughout Europe (e.g. Magny, 1993; Engels et al., 2016a). This change (Movius, 2013) coincided with a significant shift in the western Europe landscape that marked the onset of the Subatlantic period (Litt et al., 2001). The climate change 2800 years ago has been related to the occurrence of a grand solar minimum (Magny, 1993; Martin-Puertas et al., 2012b; van Geel et al., 1996; van Geel et al., 1999), the Homeric Minimum, which occurred between 2750-2550 cal years BP recognized in both ^{14}C-tree rings (Reimer et al., 2009) and ^{10}Be-Greenland ice core records(Reimer et al., 2009; Vonmoos et al., 2006). Martin-Puertas et al. (2012b) recently reconstructed changes in solar variability during the time interval from 3300 to 2000 years BP by analyzing changes in ^{10}Be accumulation rates in the annually laminated (varved) sediment record of lake Meerfelder Maar (MFM). The authors compared the reconstructed changes in solar variability to changes in

windiness (reconstructed from varve thickness) using the sediment record. The study showed a sharp increase (over less than a decade) in both the climatic and solar proxies at 2759 ± 39 varve years BP and a reduction 199 ± 9 years later, indicating that atmospheric circulation reacted abruptly and in phase with the grand solar minimum and hence showing empirical evidence for a solar-induced “Homeric Climate Oscillation” (HCO).

The HCO has been suggested to be the trigger for human migrations during the transition from Bronze Age to Iron Age (Scott et al., 2006; van Geel et al., 1996). Archeological and paleoecological studies from different locations in Europe (e.g. the Netherlands and Germany) also provide evidence for an increase in human activity and reorganization of prehistoric cultures around that time (Kubitz, 2000; van Geel et al., 1996), most likely favored by a rise in human population density after the climate deterioration (van Geel and Berglund, 2000). Although wetter conditions have been inferred for the HCO, it yet remains elusive if these wetter conditions were associated to major changes in rainfall intensity and/or lower evapotranspiration and the possible relation to the observed vegetation changes in western Europe. Furthermore, the exact temporal succession of regional hydrological and environmental changes during this period is unknown due to the lack of highly-resolved hydrological records in western Europe.

In this study we analyze high-resolution lipid biomarker hydrogen isotope ratios of a Late Holocene sedimentary sequence from lake MFM in western Germany to test its potential for elucidating the nature of hydrological changes during the HCO. Stable hydrogen isotope ratios (expressed δD values) of sedimentary lipid biomarkers (i.e. *n*-alkanes), which can be traced back to their biological sources (Eglinton and Eglinton, 2008; Killops, 2005; Peters et al., 2007; Sachs et al., 2013), have become an important paleohydrological proxy over the last ca. 15 years. This has resulted in new insights into hydroclimate dynamics over different geological timescales (Aichner et al., 2010; Atwood and Sachs, 2014; Feakins et al., 2014; Rach et al., 2014; Sachs et al., 2009; Schefuss et al., 2011; Smittenberg et al., 2011; Tierney et al., 2010; Tierney et al., 2008; Zhang et al., 2014). Rach et al. (2014)

demonstrated that *n*-alkane δD analyzes are a suitable proxy for reconstructing regional hydrological changes during major and abrupt climate shifts during the Late-Glacial that are recorded in the varved sediments of lake MFM.

Our specific objectives for this study are (1) to reconstruct hydroclimate variations for central-western Europe during a period of changing environmental conditions (3200-2000 varve years BP) using lipid biomarker stable isotope data, and (2) to combine this record with a high-resolution aquatic and terrestrial vegetation reconstruction in order to evaluate possible effects of vegetation change on the biomarker stable isotope record.

2. Lipid biomarkers as paleoclimate proxies

2.1 Sedimentary n-alkanes as biomarkers for aquatic and terrestrial organisms

Straight-chained hydrocarbons such as *n*-alkanes are increasingly applied for paleoclimate reconstruction. Different *n*-alkane homologues are produced by bacteria, aquatic as well as terrestrial plants (Aichner et al., 2010; Baas et al., 2000; Cranwell et al., 1987; Eglinton and Hamilton, 1967; Ficken et al., 2000; Gelpi et al., 1970). As such, *n*-alkanes can be used to obtain information on their biological sources. While not species-specific, different groups of source organisms can be distinguished based on *n*-alkane chain length: *n*-alkanes with 17 to 19 (nC_{17} - nC_{19}) carbon atoms (short-chain) are predominantly synthesized by aquatic algae but also by bacteria (Cranwell et al., 1987; Gelpi et al., 1970; Sachse and Sachs, 2008). Mid-chain *n*-alkanes (nC_{21} - nC_{25}) are mainly synthesized by submerged aquatic plants (Aichner et al., 2010; Baas et al., 2000; Ficken et al., 2000). Long-chain *n*-alkanes (nC_{27} - nC_{31}) are major components of the leaf waxes of terrestrial higher plants (Eglinton and Hamilton, 1967; Massimo, 1996), although conifers produce significantly smaller amounts of *n*-alkanes than broad-leaved species (Diefendorf et al., 2011). Some terrestrial plants also produce significant amounts of nC_{25}, making source assessment for this compound more difficult, but in general

aquatic or terrestrial sources can be distinguished from *n*-alkane abundances in sediments (Gao et al., 2011).

2.2. Climatic and environmental influences on δD values of aquatic and terrestrial biomarkers

The observation that δD values of aquatic (δD_{aq}) and terrestrial (δD_{terr}) plant derived lipid biomarkers record the δD values of the organisms' source water (Garcin et al., 2012; Huang et al., 2004; Sachse et al., 2012; Sachse et al., 2004; Sauer et al., 2001) has fueled the application of δD measurements as a paleohydrological proxy. The major determinant of the δD values of aquatic and terrestrial lipid biomarkers is the δD value of the source water used by the organism (Sachse et al., 2012). Photosynthetic lacustrine aquatic organisms, such as submerged aquatic macrophytes and algae use lake water as a hydrogen source to synthesize *n*-alkanes. In a closed lake system (in temperate climates), which is only fed by precipitation and characterized by a low precipitation/ evaporation ratio, the hydrogen isotope composition of lake water can be interpreted as an integrated signal of precipitation δD (Aichner et al., 2010; Sachse et al., 2012). In particular, for MFM, being a maar with steep catchment walls (sheltered from the wind) an effect of evaporation on lake water is unlikely. For a neighboring maar lake (Holzmaar) a long-term study of lake water has shown that $\delta^{18}O$ values vary only around 1‰ and follow the seasonal temperature evolution (Moschen et al., 2005). Thus, in such a lake system sedimentary δD_{aq} values provide an integrated precipitation δD signal (Sachse et al., 2004).

Higher land plants on the other hand directly take up precipitation water (through soil water) (Sachse et al., 2012). However, transpirative processes in the leaf of the plant modify the isotopic composition of water (i.e. increased enrichment in D under drier conditions) before hydrogen is being fed into biosynthetic reactions (Kahmen et al., 2013a; Kahmen et al., 2013b; Sachse et al., 2012). As a consequence, sedimentary δD_{terr} values also record changes in ecosystem evapotranspiration (Kahmen et al., 2013b; Sachse et al., 2004).

191

192 *2.3. Species-specific differences and their influence on aquatic and terrestrial*
193 *lipid δD values*

194 In addition to the isotopic composition of source water, it has been
195 demonstrated that changes in vegetation type (of terrestrial plants) as well as
196 aquatic lipid source organisms can also significantly affect the isotope
197 composition of terrestrial and aquatic lipids (Sachse et al., 2012).
198 For example, major differences in the net or apparent fractionation ($\varepsilon_{l/w}$), i.e.
199 the isotopic difference between the source water (δD_w) and lipid (δD_l) (equ. 1),
200 have been observed among different plant functional types (Gao et al., 2014;
201 Sachse et al., 2012).
202

$$(1) \quad \varepsilon_{l/w} = \frac{(D/H)_l}{(D/H)_w}$$

203

204 Since $\varepsilon_{l/w}$ represents the sum of physical and biochemical fractionation
205 processes, it is currently unclear to what extent individual parameters are
206 responsible for the observed differences. For example, major differences in
207 the biosynthetic fractionation (ε_{bio}) between various species as well as
208 differences in leaf-morphology, transpiration and water use efficiency between
209 grasses and broadleaf-woody plants have been shown to affect $\varepsilon_{l/w}$ (Kahmen
210 et al., 2013b; Liu et al., 2006; McInerney et al., 2011; Sachse et al., 2012).
211 On the other hand, $\varepsilon_{l/w}$ in aquatic algae and cyanobacteria can also be
212 influenced by water salinity and growth rate, possibly related to biochemical
213 processes as shown for *n*-alkanoic acids (Sachs, 2014), the biosynthetic
214 precursors of *n*-alkanes (Eglinton and Eglinton, 2008; Sachse et al., 2012;
215 Sessions et al., 1999). In addition, significant differences in ε_{bio} have been
216 observed among different algae (Zhang and Sachs, 2007). For example,
217 under similar conditions in batch cultures, two different groups of green algae
218 (Chlorophyceae and Trebouxiophyceae) produced C_{16} *n*-alkanoic acids, which
219 differed in their δD values by 160‰ (Zhang and Sachs, 2007). Less
220 information is available for submerged aquatic plants, but studies on modern

aquatic plants and lake surface sediments have suggested the ε_{bio} for aquatic macrophytes (i.e. *Potamogeton*) may be significantly smaller (-82‰) (Aichner et al., 2010) than observed for algae (-157‰) (Sachse et al., 2004). Therefore, if various algae and other water plants produce the same unspecific biomarker (e.g. short- to mid-chain *n*-alkanes) and the aquatic ecosystem (i.e. species composition) changes, the sedimentary *n*-alkane δD record could be affected. In a similar way, major vegetation changes can affect the δD_{terr} signal (Nelson et al., 2013). Despite these complications, δD values of aquatic and terrestrial lipids from sedimentary archives can be used to reconstruct changes in hydroclimate over time, if constraints on the processes discussed above, i.e. information about the terrestrial and aquatic producers of the studied lipids, are available (Aichner et al., 2010; Atwood and Sachs, 2014; Rach et al., 2014).

Therefore, for a robust paleoclimatic interpretation it is important to understand the interplay between hydrological and vegetation change and their effect on sedimentary lipid biomarker δD records. The here studied time interval was characterized by long and short-term climatic change as well as vegetation changes and this provides a testing ground to study the above discussed processes and their influence on biomarker δD values. Therefore, we compare a high-resolution δD_{aq} and δD_{terr} record from lake MFM in western Germany to lake and catchment ecosystem development, inferred from a new pollen-based vegetation reconstruction, as well as published sedimentary proxy data from MFM, such as varve thickness and Ti influx (Martin-Puertas et al., 2012b).

3. Study site

Lake Meerfelder Maar (*50° 06‘ 2.87“ N; 06° 45‘ 27.13“ E*) is located in western Germany as a part of the West-Eifel Volcanic Field (Fig. 1). The lake is situated in a volcanic crater which was formed by a phreatomagmatic eruption 80,000 years ago (Zöller, 2009).

The modern lake is situated at 336.5 m a.s.l. and the lake surface is around 0.248 km^2, covering the northern part (ca. 1/3) of the maar crater surface (Fig. 1). The maximum water depth is 18m. The southern part of the crater is filled in by a shallow delta plain, deposited from a stream (Meerbach) passing through the crater rim in the south. The lake is eutrophic and due to its particular morphological situation within a deep maar crater, Lake MFM is wind-sheltered, favoring the preservation of fine seasonal layers within the sediment sequence (Brauer et al., 1999a; Brauer et al., 2008).

The climate of the region is influenced by its proximity to the North Sea coast (ca. 250 km) with a mean annual air temperature of 8.2 ºC and mean annual precipitation of 950 mm, peaking in winter (Martin-Puertas et al., 2012a).

Seven sediment cores were collected in 2009 from the deepest area of Lake MFM using a UWITEC piston core, with a maximum distance between sites of 20 m. The sediment cores, labeled as MFM09-A to MFM09-G, were split, imaged, described and an overlapping sediment profile was constructed (Martin-Puertas et al., 2012a). For the present study the uppermost core MFM09-A was selected for sampling. We studied a meter long sequence from 230 to 330 cm depth, which covers the interval from 2000 to 3200 varve years BP (Martin-Puertas et al., 2012b). The MFM chronology (MFM2000) has been established by varve counting from ca. 1500 cal years BP back to 14,200 cal years BP along 7.85 m of sediments with a cumulative counting error of less than 5% and is supported by 51 radiocarbon dates (Brauer et al., 2000). This independent but floating chronology was anchored to the calendar year time scale by adopting the age of the regional (Eifel) Ulmener Maar Tephra (UMT) for the MFM record (Brauer et al., 1999b; Brauer et al., 2000). The UMT is dated at 11,000 ± 110 cal years BP in the Lake Holzmaar (HZM) varve chronology by multiple count sequences and ^{14}C based-correction (Zolitschka et al., 2000). The proximity of Lake HZM to MFM (10 km) provides the opportunity to compare both records, showing a good agreement between the chronologies (Litt et al., 2009). For the study interval, an age error estimate has been provided by combining varve counting, radiocarbon dating and sediment ^{10}Be accumulation rates (Martin-Puertas et al., 2012b). All ages in

the following text are rounded on 5 years to avoid interpretations on a temporal accuracy level, which is not supported by the current age model.

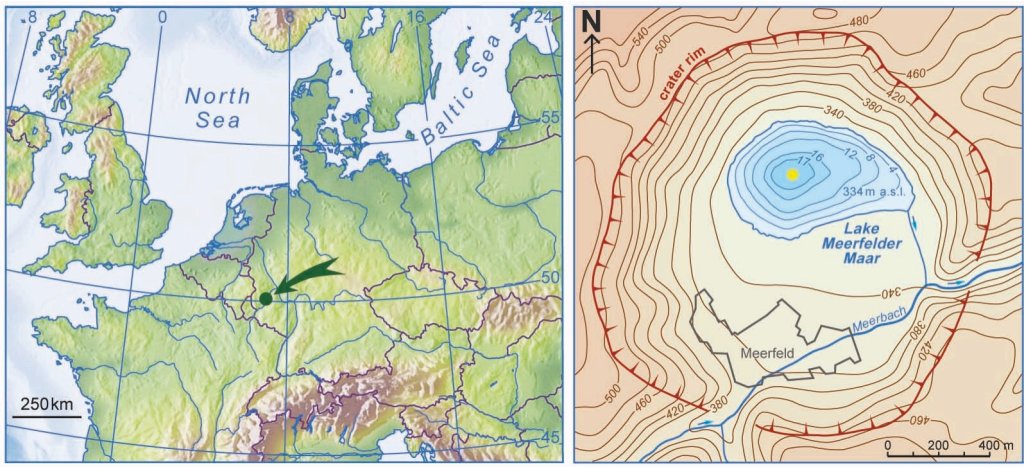

Fig. 1: Map of western Europe with the study locations. Coloured dots mark the study (left) and coring (right) site at MFM.

4. Methods

4.1 Biomarker extraction, identification and quantification

A 1.0-m-long core section, which included the time interval of the HCO, was sampled in consecutive 1-cm-thick slices, resulting in a total of 100 samples. Due to differences in sedimentation rate, the temporal resolution of the samples varies between 4 and 45 years per sample.

To remove remaining water, all samples were freeze-dried and subsequently homogenized. A Dionex accelerated solvent extraction system (ASE 350) with a dichloromethane (DCM): methanol mixture (9:1) at 100°C and 103 bar was used for the extraction of lipid biomarkers from freeze-dried samples in the biomarker laboratory at the University of Potsdam. The total lipid extracts (TLE) were separated into three fractions (aliphatic (F1), aromatic (F2) and alcohol/ fatty acid (F3)) by solid phase extraction (SPE). The separation was achieved using 2g silica gel as the stationary phase and hexane, hexane:DCM (1:1) and DCM as the respective mobile phases. Activated copper in a pipette column was used to remove elemental sulfur from the F1 fraction. The aliphatic fraction was dominated by *n*-alkanes (nC_{21}-nC_{31} homologues) and alkenes. Fractions F2 and F3 contained mainly ketones, alcohols and fatty acids. To avoid coelution of alkanes and alkenes during

isotope measurement, the F1 fraction was further purified using silver nitrate ($AgNO_3$) impregnated silica gel in a pipette column with hexane and dichloromethane as the mobile phase for the elution of alkanes and alkenes, respectively.

n-Alkane identification and quantification was performed using a gas chromatograph (GC 7890-A, Agilent, Santa Clara, USA) coupled to a flame ionization detector (FID) and a mass selective detector (MSD) (MS 5975-C, Agilent, Santa Clara, USA) coupled via an electronic split interface. The quantification was performed through the FID by comparing compound peak area to the peak area of the internal standard (5α-androstane). Compound identification was achieved using the MSD and comparison with library and literature mass spectra. The GC temperature program used for *n*-alkane quantification contained the following specifications: injection at 70°C (hold for 2 minutes), then heating up to 140°C with a ramp of 12°C per minute directly followed by a heating to 320°C with a ramp of 2°C per minute. The final temperature of 320°C was held for 15 minutes. The PTV injector started at 50°C and was heating up to 350°C with a ramp of 14°C per second.

4.2 Stable isotope measurement and evaluation

Compound-specific hydrogen isotope ratios of the *n*-alkanes were measured on a Delta-V-Plus Isotope Ratio Mass Spectrometer (IRMS) (Thermo Fisher, Bremer, Germany) coupled to a Trace Gas Chromatograph Ultra (Thermo Fisher, Bremer, Germany) at the Swiss Federal Institute of Technology Zurich (ETH Zurich). The following GC-temperature program was used: start at 90°C (held for 2 minutes), heating up to 150°C with 10°C per minute, heating from 150°C to 320°C with 4°C per minute; the final temperature was held for 10 minutes. Each sample was injected three times. For conversion of the measured δD values to the VSMOW scale a standard containing nC_{16} to nC_{30} alkanes (Mix A4 obtained from Arndt Schimmelmann, Indiana University) with known δD values was measured in triplicate at the beginning and the end of each sequence. All measured δD values were corrected to the VSMOW scale using a linear regression function (with a specific slope and intercept) derived

from measured vs. real Mix A4 standard values. The mean standard deviation of all A4 standard measurements (n=441) was 2.1‰, while the mean standard deviation of all sample *n*-alkane measurements (n=492) was 1.4‰. To avoid misinterpretation of the measured δD values only baseline separated peaks with areas over 20Vs have been used for interpretation. The $H3^+$ factor was determined before each sequence and remained constant at 3.63 ± 0.39 during the 4 weeks measurement period.

4.3 Palynological analysis

Two plastic containers of 35x260 mm were pressed into cores MFM09A2DR and MFM09A2UR to a depth of 10 mm. The sediment in the plastic containers was subsequently subsampled with a 3 samples/ centimeter resolution for the sediments older than 2765 varve years BP and a 2 samples/ centimeter resolution for the sediments younger than 2765 varve years BP. These sampling intervals correspond to a temporal resolution of 1-29 years per sample. Ninety-one samples were prepared for the analysis of pollen and spores at the University of Amsterdam following the protocols of Faegri et al. (1990) and Moore et al. (1991). Standard tablets with *Lycopodium* spores were added to the sample during laboratory processing to estimate pollen and spore concentrations and influx numbers (Stockmarr, 1971). Pollen, fern spores, fungal spores, and other palynomorphs (including remains of freshwater algae) were identified using a light microscope with 400× magnification (1000× when necessary). Keys and illustrations by Moore et al. (1991) and Beug (2004) as well as a reference collection were used for pollen identification. The identification of algal remains and other non-pollen palynomorphs (NPPs) follows van Geel (1978). A pollen percentage diagram was calculated using a pollen sum (Σ-pollen) that includes arboreal pollen and pollen of upland herbs and the average Σ-pollen is 572 (range: 443-698). The percent-abundances of all pollen, spores and NPPs are calculated in relation to Σ-pollen. Concentrations of individual taxa were calculated by multiplying the number of encountered pollen by the ratio of the number of added *Lycopodium* spores and the number of spores encountered during analysis.

This number was then divided by the volume of material used in the analysis to derive taxon-specific pollen concentrations. A percent-abundance diagram was plotted using TILIA v 1.17.6; concentration- and influx-diagrams were plotted using C2. Details on the taxa important for the interpretation of our *n*-alkane data are presented in section 5.3 (pollen data), whereas overview diagrams of the arboreal taxa (percentages, concentrations and influx) (Fig. S1) and the aquatic taxa (expressed as percentages in relation to Σ-pollen) (Fig. S2) can be found in the Supplementary Information.

5. Results

5.1 n-Alkane concentrations

In total 100 samples were analyzed for their *n*-alkane content. Eighteen samples did not contain enough material for *n*-alkane analysis. In the remaining 82 samples the concentration of all identified *n*-alkanes (nC_{21} to nC_{31}) ranged from 0.34 to 69.42μg/g dry weight of sediment. The most abundant *n*-alkane homologue in all samples was nC_{29} with an average concentration of 26.5μg/g sediment dry weight per sample (range 3.0-69.1μg/g). The compound with the lowest concentration was always nC_{21} with 3.9μg/g on average (range 0.34 -14.3μg/g). Other *n*-alkanes (nC_{23}, nC_{25}, nC_{27} and nC_{31}) had average concentrations between 4.2 to 20.5μg/g sediment dry weight. The average chain-length (ACL) varied between 26.0 and 28.8.
The average influx values (μg normalized per varve year) of short- and long-chain *n*-alkanes showed significant variations. Before the HCO, nC_{21} and nC_{23} showed average influx values of 0.35 and 0.27μg/ year, while the nC_{25} to nC_{31} homologues showed average influx values between 0.46 and 1.34μg/year, respectively (Fig 2B). The influx of nC_{21} and nC_{23} increased rapidly to 0.68 and 1.03μg/ year after 2785 varve years BP, while the influx values of nC_{25} to nC_{31} also increased to average values between 2.10 and 6.28μg/year (Fig 2B). The average *n*-alkane influx values for nC_{21} and nC_{23} decreased abruptly to average values of 0.12 and 0.15μg /year after the HCO (Fig 2B). The nC_{25}

405 to nC_{31} homologues also decreased to average influx values between 0.37
406 and 1.42μg/ year. nC_{21} showed maximum influx values during the first part of
407 the HCO (2750 – 2660 varve years BP), while long-chain *n*-alkanes had their
408 maximum influx rates in the second part of the HCO (2700 – 2610 varve years
409 BP) (Fig 2B). Influx rates of nC_{23} showed local maxima both in the first half of
410 the HCO (at 2740 varve years BP) as well as in the second half of the HCO
411 (at 2610 varve years BP) (Fig 2B).
412
413 *5.2 Stable hydrogen isotope composition (δD values) of the n-alkanes*
414 All 82 samples were analyzed for compound specific stable hydrogen isotope
415 ratios, expressed as δD values. The *n*-alkane δD values showed a
416 decreasing trend during the analyzed period (Fig 2A). Generally, the δD
417 values of all *n*-alkanes were more positive before the HCO than after (Fig 2A).
418 However, there were major differences in the magnitude of variation between
419 *n*-alkanes of different chain-length. Short and mid-chain *n*-alkanes (nC_{21}-nC_{25})
420 generally showed higher variability in their δD values than long-chain *n*-
421 alkanes. Before the HCO, nC_{21} δD values were on average -135 ± 2‰
422 (arithmetic mean from 3190 to 2785 varve years BP with respective 95%
423 confidence interval) while after the HCO the average δD value changed to -
424 160 ± 5‰ (arithmetic mean from 2540 to 2015 varve years BP). Applying the
425 epsilon equation (Sessions and Hayes, 2005) for accurate calculations of
426 differences in δ-values results in a difference of about 30‰ for nC_{21} δD values
427 before and after the HCO. The average δD values of nC_{23} and nC_{25} for the
428 same period changed from -153 ± 3‰ and -152 ± 3‰ to -171 ± 7‰ and -176
429 ± 4‰, respectively (difference 22 and 28‰) (Fig 2A).
430 Long-chain *n*-alkanes generally showed smaller changes in their δD values.
431 The average δD values of nC_{27} and nC_{29} changed from -169 ± 2‰ and -188 ±
432 2‰ (before the HCO) to -182 ± 3‰ and -192 ± 2‰ (after the HCO) (difference
433 15 and 4‰). The δD values of nC_{31} changed from -162 ± 3‰ to -179 ± 2‰
434 (difference 20‰) (Fig 2A).
435

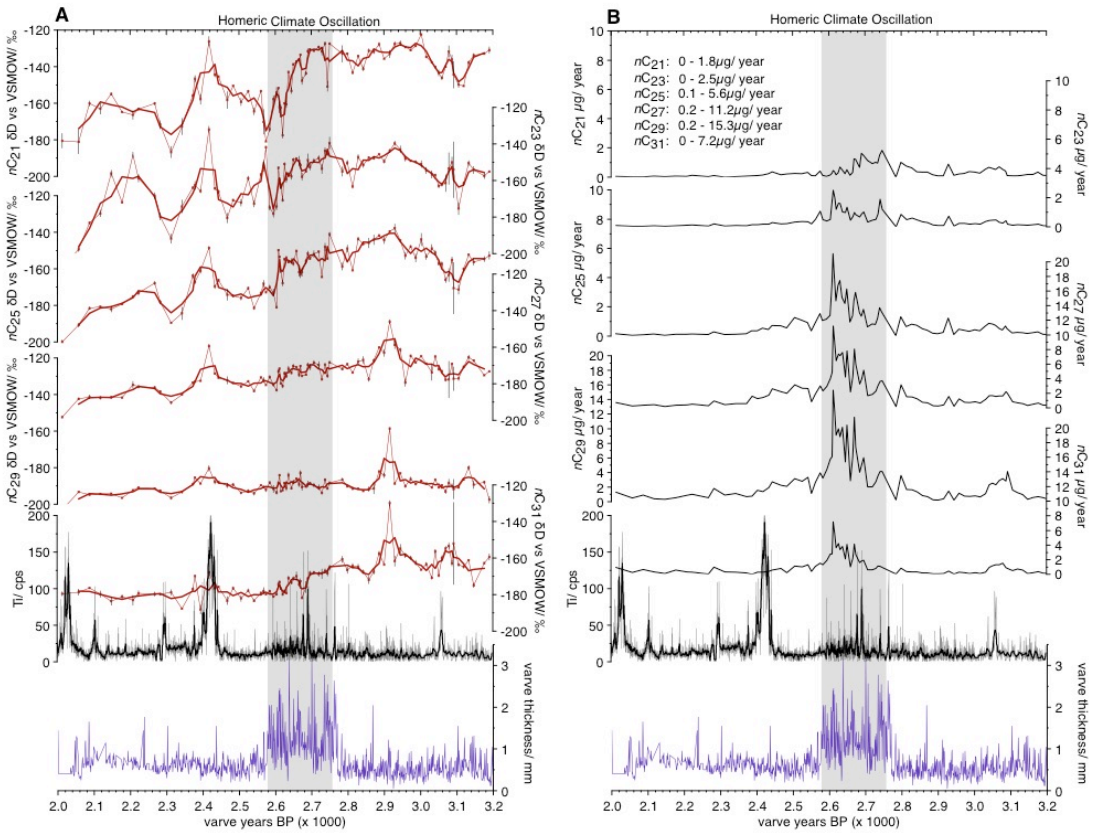

Fig. 2: δD values (A) (smoothing by 3-data running average) and annual flux (*µ*g/ year) (B) of nC$_{21}$-nC$_{31}$ alkanes and varve thickness as well as Titanium content (smoothing by 100-data running average) (Martin-Puertas et al., 2012b) of the studied core section.

5.3 Pollen-data

The lower part of the pollen record (2945-2795 varve years BP) was characterized by relatively high percentages of arboreal pollen (AP) of 95-100% (Fig. 3). The pollen-assemblages were dominated by *Fagus* which reached abundances >60%, accompanied by relatively high abundances of other deciduous tree taxa such as *Alnus* (15-30%), *Corylus* (5-15%) and *Quercus* (5-15%). Pollen from non-arboreal taxa (NAP) were only present in low abundances between 2945-2795 varve years BP, suggesting that the vegetation around MFM consisted of a closed-canopy forest.

A sharp decrease in relative abundance of *Fagus* to values of around 40% was observed at ~2795 varve years BP (Fig. 3). Simultaneously, spores of *Kretzschmaria deusta*, a parasitic fungus living on various tree species (van

Geel et al., 2013), showed an increase in abundance to values of 5%. An increase in the relative abundance of *Alnus* as well as of several NAP-taxa coincided with the decrease in *Fagus* (Fig. 3). Crop plants (e.g. Poaceae, Cerealia) as well as *Plantago lanceolata* and *Rumex acetosella-type* all started to increase after 2795 varve years BP. Remains (vegetative cell walls) of the green algae *Botryococcus*, *Tetraedron minimum* and of the aquatic macrophyte *Myriophyllum spicatum*/*verticillatum*-type showed an increase around 2620 and 2595 varve years BP, respectively.

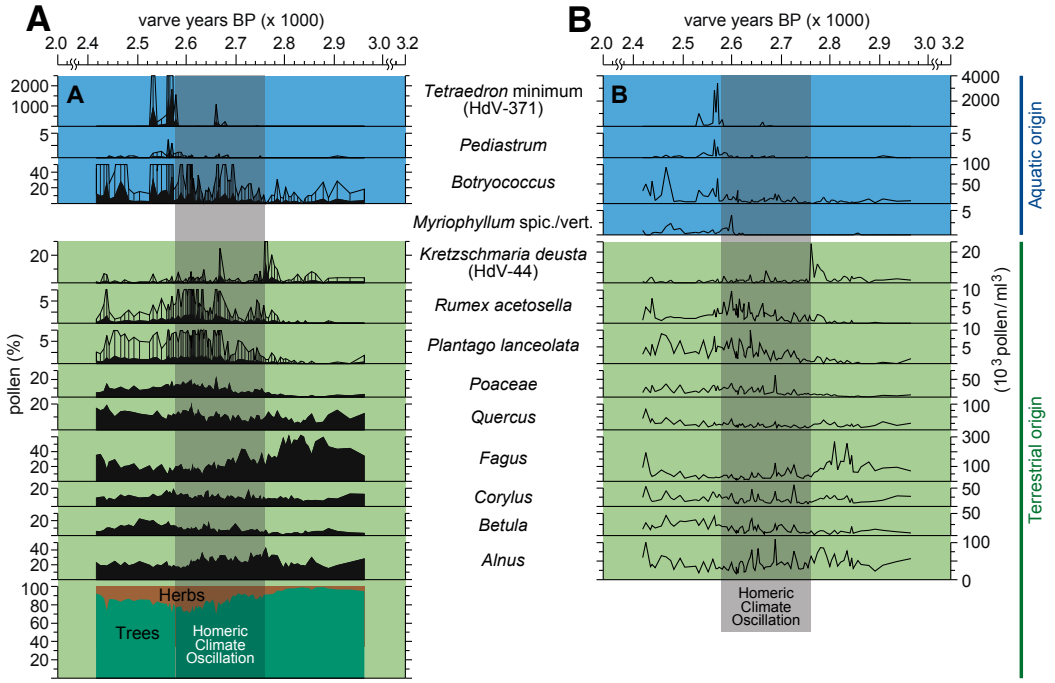

Fig. 3: Pollen and spores abundance of the major constituents of vegetation in and surrounding MFM given in % (A) and pollen concentrations (B). Thinner lines on top of the upper six plots in A marking exaggeration-lines (5-times). Blue shaded areas marking aquatic organisms. Green areas are showing terrestrial plants. The dark-green/ orange areas show the local tree/ herb distribution in percentage.

6. Discussion

Our lipid biomarker stable hydrogen isotope record showed a long-term trend to more negative δD values during the 3200 to 2000 varve years BP interval. This is evident in all analyzed biomarkers, regardless of their biological origin

475 (Fig. 2). The decrease in lipid δD values possibly reflects the long-term
476 cooling trend as a consequence of declining summer insolation in the
477 Northern Hemisphere (Marcott et al., 2013; Renssen et al., 2009) in the way
478 that a decrease in air temperature would lead to more negative precipitation
479 δD values (Dansgaard, 1964; Gat, 1996; Gat et al., 2000). However, we
480 observed substantial differences in the magnitude of changes in δD values
481 between aquatic and terrestrial plant derived lipid biomarkers: δD_{aq} values
482 showed a rather abrupt decrease starting at around 2700 varve years BP, a
483 change not observed for δD_{terr} values (except a slight decrease in $n C_{31}$ δD
484 values). This indicates that different processes controlled the observed
485 changes for aquatic and terrestrial biomarkers. While different biosynthetic
486 fractionation factors for aquatic and terrestrial plants can explain different
487 absolute δD values, different magnitudes of change indicate either significant
488 evapotranspirational or ecological changes. For example, cooler and more
489 arid conditions could explain a stronger decrease in δD_{aq} compared to δD_{terr},
490 as δD_{terr} values would reflect increasing plant transpiration (Kahmen et al.,
491 2013b). However, there is no evidence for a substantial aridification during
492 this period in western Europe. Rather, several studies suggest a shift to more
493 humid conditions during this period (Martin-Puertas et al., 2012b; van Geel,
494 1978; van Geel et al., 1996; van Geel et al., 2013). With our combined high-
495 resolution lipid biomarker and palynological analysis we therefore explore
496 ecological changes in the aquatic and terrestrial ecosystem in and around
497 MFM to test if these changes may have influenced the magnitude of change
498 in biomarker δD values.
499
500 *6.1. Changes in vegetation based on palynological records*
501 The palynological data provide first evidence for changes in the terrestrial
502 ecosystem at ca. 2800 varve years BP. Our pollen record showed a decrease
503 in relative pollen abundance of *Fagus* by half and a doubling of *Alnus,*
504 accompanied by a general trend to increasing grass/herb vegetation in the
505 catchment of MFM (Fig. 3A). The presence/increase of human-impact
506 indicators such as *Plantago lanceolata* and *Rumex acetosella*-type provided

507 evidence for increased human impact (Behre, 1981) in the catchment of MFM.
508 *Kretzschmaria deusta* spores increased in abundance from 2795 to 2765
509 varve years BP, which could be a result of the temporary occurrence of this
510 fungus on wounded trees that were present in the landscape after the clearing
511 of parts of the forest (Kubitz, 2000; van Geel et al., 2013).
512 The second substantial decline in tree pollen at 2695 varve years BP occurred
513 about 100 years after the variations mentioned above (Fig 3A). This marks a
514 second phase of ecosystem changes, which is additionally characterized by
515 an increase of *Botryococcus* – green algae (Fig 3A). This second phase in
516 ecological change could even have been caused by further increased human
517 impact but climatic changes cannot be ruled out either.
518
519 *6.2. Environmental and hydroclimatic changes inferred from changes in lipid*
520 *biomarker abundance and δD values*
521
522 *6.2.1 Terrestrial biomarker flux into the sediment*
523 At 2695 varve years BP, about 60 years after the increase in varve thickness
524 (Fig 2) (Martin-Puertas et al., 2012b), our lipid biomarker record showed an
525 increased influx of leaf wax *n*-alkanes into the sediment (Fig 2B). This
526 doubling in lipid biomarker flux occurred simultaneous with an increase in
527 Titanium counts, a proxy for surface runoff (Fig. 2) (Martin-Puertas et al.,
528 2012b). At the same time, tree pollen decreased significantly (from 90-71%)
529 and grass and other herbaceous pollen increased from 10 to 29% (Fig. 3A).
530 We interpret these changes in the pollen record to reflect a shift toward a
531 more open landscape, which might have led to increased erosion and flux of
532 terrestrial material into the lake. This is supported by the observation that the
533 influx of terrestrial biomarkers reached its maximum at the same time when
534 the tree / herb pollen ratios showed their lowest value at ca. 2610 varve years
535 BP. However, the onset of the tree pollen decline (from 96-86%) and
536 increasing grass pollen (from 4 to 14%) occurred already 100 years earlier, at
537 ca. 2800 varve years BP. Also, varve thickness increased likely because of

windier conditions already ca. 60 years before the increased terrestrial lipid biomarker influx at 2760 varve years BP.

The decadal resolution of our lipid biomarker and palynological data allows a detailed assessment of the temporal succession of proxy changes related to the HCO. We have to note that the different vegetation proxies presented here (alkanes, pollen) partly may reflect different source areas. While most of the *n*-alkanes likely were derived from vegetation growing on the lake shore, pollen assemblages may also include a signal from the upland vegetation surrounding the MFM crater. However, the specific catchment-conditions of lake MFM, with its steep crater walls and small catchment area, make it most likely that most pollen is derived from the catchment vegetation itself, and that the contribution of long distance transport is of minor importance (Engels et al., 2016b; Litt et al., 2009). The initial change in the pollen diagram observed at ca. 2800 varve years BP is not linked to additional transport of terrestrial material into the lake. Only at ca. 2700 varve years BP, when the largest vegetation change occurred, soil erosion increased. The first decrease in pollen concentrations at 2800 varve years BP may be due to decreased pollen production as a result of increased ecological stress, instead of changes in vegetation, which may have followed a few decades later.

6.2.2 Biomarker δD values as recorders of hydroclimate

In addition to the long-term trend to more negative δD values between 3200 and 2000 varve years BP (Fig. 2A), evident in nearly all analyzed biomarkers (except nC_{29}), aquatic and terrestrial lipid biomarker δD values showed their most substantial decrease (by between 30 and 4‰) during the HCO interval (Fig. 4).

While the 4-20‰ decrease in δD_{terr} values could have been caused by a combination of cooler conditions and lower plant transpiration (Craig, 1965; Flanagan et al., 1991; Kahmen et al., 2013b; Sachse et al., 2012) under the more humid conditions suggested by earlier studies (van Geel et al., 1996), it

remains difficult to explain the rapid decline in δD_{aq} values between 22-30‰, as these would not be affected by changes in terrestrial transpiration. While a decrease in air temperature would lead to more negative precipitation δD values, the observed decrease of 22-30‰ in δD_{aq} would imply an unrealistic temperature decrease between 11 and 15°C during the HCO, when considering the modern temperature sensitivity of precipitation δD in this region (2‰/°C; (IAEA/WMO, 2006)). While no temperature reconstructions are available for the HCO, a temperature decrease between 0.5-1.5°C has been suggested for similar solar minima (Martin-Puertas et al., 2012b). Therefore, a potential 0.5-1.5°C decrease during the HCO would only have had a minimal effect on precipitation δD values. However, a decrease in temperature may also be associated to shifts in the moisture source region and/or changes in moisture source temperature, which may have exercised additional control on decreasing δD values. For example, Martin-Puertas et al. (2012b) suggested a reduced atmospheric pressure gradient between the subtropics and Iceland for the HCO, resembling a negative phase of the North Atlantic Oscillation (NAO), which today results in more negative winter δD_{precip} values in parts of western Europe (Baldini et al., 2008). However, we do not observe an increase in δD values after the HCO, suggesting the observed change was not an excursion or phase but rather a shift of atmospheric conditions to a new regime.

While the relatively small changes in δD_{terr} can be largely explained by the proposed long-term hydroclimatic changes during this period, the abrupt changes in δD_{aq} of up to 30‰ over 180 years are difficult to reconcile with this scenario. Due to the absence of other proxy indicators suggesting hydroclimatic changes that could explain such a decline in δD_{aq}, we explore the possibility that factors additional to hydroclimate influenced δD_{aq}.

6.2.3. The effect of lake ecosystem changes on δD values of aquatic n-alkanes

Additional factors known to affect δD_{aq} include changes in water salinity, light intensity, growth rate and species changes (Sachs, 2014; Zhang and Sachs,

601 2007). MFM always was a freshwater lake, so that we can rule out salinity as
602 a driver. Increased upland erosion and a subsequent delivery of nutrients into
603 the lake may have resulted in increasing growth rates of aquatic organisms.
604 However, for aliphatic lipids produced by algae D/H fractionation does not
605 seem to change significantly with growth rate (Sachs, 2014), and no such
606 data exist for aquatic plants.
607 However, palynological data indicate significant changes in the aquatic
608 ecosystem at 2625 varve years BP, when the total amount of aquatic and
609 swamp taxa pollen/ remains started to increase from virtually zero to a
610 maximum of 1.5% at 2600 varve years BP (Fig. 4). Strikingly, this increase, as
611 well as the change in species composition, was synchronous to the largest
612 changes in nC$_{21}$ and nC$_{23}$ alkane δD values (Fig 4). These compounds are
613 primarily synthesized by aquatic organisms, likely aquatic macrophytes
614 (Aichner et al., 2010; Cranwell et al., 1987). A minor decrease was also
615 observed for nC$_{25}$ δD (Fig 2) values, a compound that can originate from both
616 aquatic as well as terrestrial sources (Baas et al., 2000; Eglinton and
617 Hamilton, 1967; Ficken et al., 2000). Palynological analysis indicates the
618 occurrence / increase of *Myriophyllum spicatum*/*verticillatum-type (*submerged
619 aquatic plant)*, Botryococcus*, *Pediastrum* and *Tetraedron minimum* (green
620 algae) during and after the HCO (Fig. 3). The most abundant aquatic taxon
621 identified from the microfossil record is *Botryococcus* (identified by vegetative
622 cell walls). As such, the available palynological data indicate major changes in
623 the aquatic ecosystem at 2625 varve years BP, coeval with the largest
624 change in δD_{aq} values. Since nC$_{21}$ and nC$_{23}$ alkanes can be produced by a
625 variety of different algae and submerged aquatic macrophytes (Aichner et al.,
626 2010; Ficken et al., 2000; Gelpi et al., 1970; Parrish, 1988) it is possible that a
627 change in the predominant aquatic organisms, characterized by different
628 magnitudes of ε_{bio}, was at least partly responsible for the observed changes.
629 For the more ubiquitous nC$_{16}$ alkanoic acid differences in ε_{bio} of up to 160‰
630 between different green algal taxa have been observed in culture studies
631 (Zhang and Sachs, 2007). As such, if the spectrum of organisms producing
632 nC$_{21}$ and nC$_{23}$ was relatively small, which is supported by the limited number

633 of pollen of aquatic taxa (Fig 3), it is conceivable that changes in the
634 predominant nC$_{21}$ and nC$_{23}$ producers have resulted in a significant variation
635 within the sedimentary δD_{aq} record.
636 Therefore, we argue that the change in the δD values of the nC$_{21}$ and nC$_{23}$
637 alkanes does not only reflect hydroclimatic changes, but that it was amplified
638 as a result of a change in aquatic lipid sources. This also implies that without
639 knowledge of the biosynthetic fractionation factors for the individual nC$_{21}$ and
640 nC$_{23}$ producers, a direct reconstruction of source water δD values is
641 impossible. Arguably, the observed changes in the aquatic ecosystem were
642 most probably initiated by the climatic and environmental changes. We
643 suggest that the increasing influx of terrestrial material between 2695 and
644 2610 varve years BP due to wetter conditions and decreasing tree cover (see
645 section 6.2.1), delivered more nutrients into the lake, acting as a fertilizer for
646 aquatic plants. The increase in abundance of aquatic organisms around 2640
647 varve years BP occurred 60 years after the increase of terrestrial biomarker
648 flux into the lake, possibly marking a threshold in the fertilization rate and
649 triggering the diversification of the aquatic ecosystem.
650
651 *6.2.4. The effect of vegetation changes on δD values of terrestrial n-alkanes*
652 δD values of the terrestrial plant derived nC$_{27}$, nC$_{29}$ and nC$_{31}$ *n*-alkanes
653 decreased in total by 15, 4 and 20‰, respectively, during the HCO interval
654 (difference between mean δD values from before and after the HCO) (Fig 2).
655 While changes in nC$_{27}$ and nC$_{29}$ δD values were gradual and can be
656 explained by hydroclimatic changes (i.e. cooler and more humid conditions),
657 the first larger and relatively abrupt decrease within the HCO of about 7‰
658 observed for nC$_{31}$ at 2685 varve years BP coincides with the onset of a 20%
659 increase in grass and other herbaceous pollen (Fig 3) likely caused by an
660 increase of human impact (Kubitz, 2000). As such, the change in δD values of
661 nC$_{31}$ may have been amplified by changes in terrestrial vegetation and
662 influenced not only by climatic but also by anthropogenic factors. While nC$_{31}$
663 is produced by different tree species (e.g. *Betula, Acer* (Diefendorf et al.,
664 2011)) it is often found in higher concentrations in grasses (Massimo, 1996).

Therefore, the more negative δD values after 2680 varve years BP may reflect at least partly the increased amount of grass-derived nC_{31} into the lake sediment, as *n*-alkane δD values from grasses are usually found to be more negative (up to 30‰) compared to those from trees (Duan and He, 2011; Hou et al., 2007; Kahmen et al., 2013b; Liu et al., 2006; Sachse et al., 2012). Based on the palynological data we suggest that the nC_{27} and nC_{29} alkanes in the MFM sediments were primarily produced by trees such as *Alnus*, *Betula*, *Salix*, *Fagus*, *Carpinus*, *Ulmus* and *Quercus*, species known to produce the *n*-alkanes (Diefendorf et al., 2011; Piasentier et al., 2000; Sachse et al., 2006). Interestingly, nC_{29} δD values from the MFM sediments of the analyzed period were on average 18‰ more negative than nC_{27} and nC_{31} δD values. This consistent offset possibly implies a different water source or a different ε_{bio} for all or the major nC_{29} source organisms. The pollen record provides evidence for a high proportion of *Alnus* and *Salix* in the catchment area, taxa primarily adapted to wetter areas such as lake shores and riversides (Landolt and Bäumler, 2010; Lauber and Wagner, 2001). *Alnus* and *Salix* have been found to synthesize higher amounts of nC_{29} (Diefendorf et al., 2011; Sachse et al., 2006) and therefore the more negative nC_{29} δD values may be due to the preferred location at the lakeshore within the crater, where higher relative humidity (due to the proximity of the water body) may have resulted in smaller leaf water isotope enrichment (Craig, 1965; Farquhar et al., 2007; Flanagan et al., 1991; Kahmen et al., 2011; Kahmen et al., 2013b).

Due to the wide variety of possible sources of the nC_{27} and nC_{29} alkanes, it is likely that these compounds had the highest integrative capacity and the occurrence or disappearance of single species did not significantly affect the sedimentary δD record. As such δD values of these compounds more faithfully recorded the long-term late Holocene hydroclimatic trend to cooler and wetter conditions. Nevertheless, while less susceptible to changes than species-poor assemblages, major environmental perturbances such as human impact on vegetation, wildfires, etc, can significantly affect diverse and species-rich plant assemblages to the extent that *n*-alkane records (and their stable isotope records) can be affected.

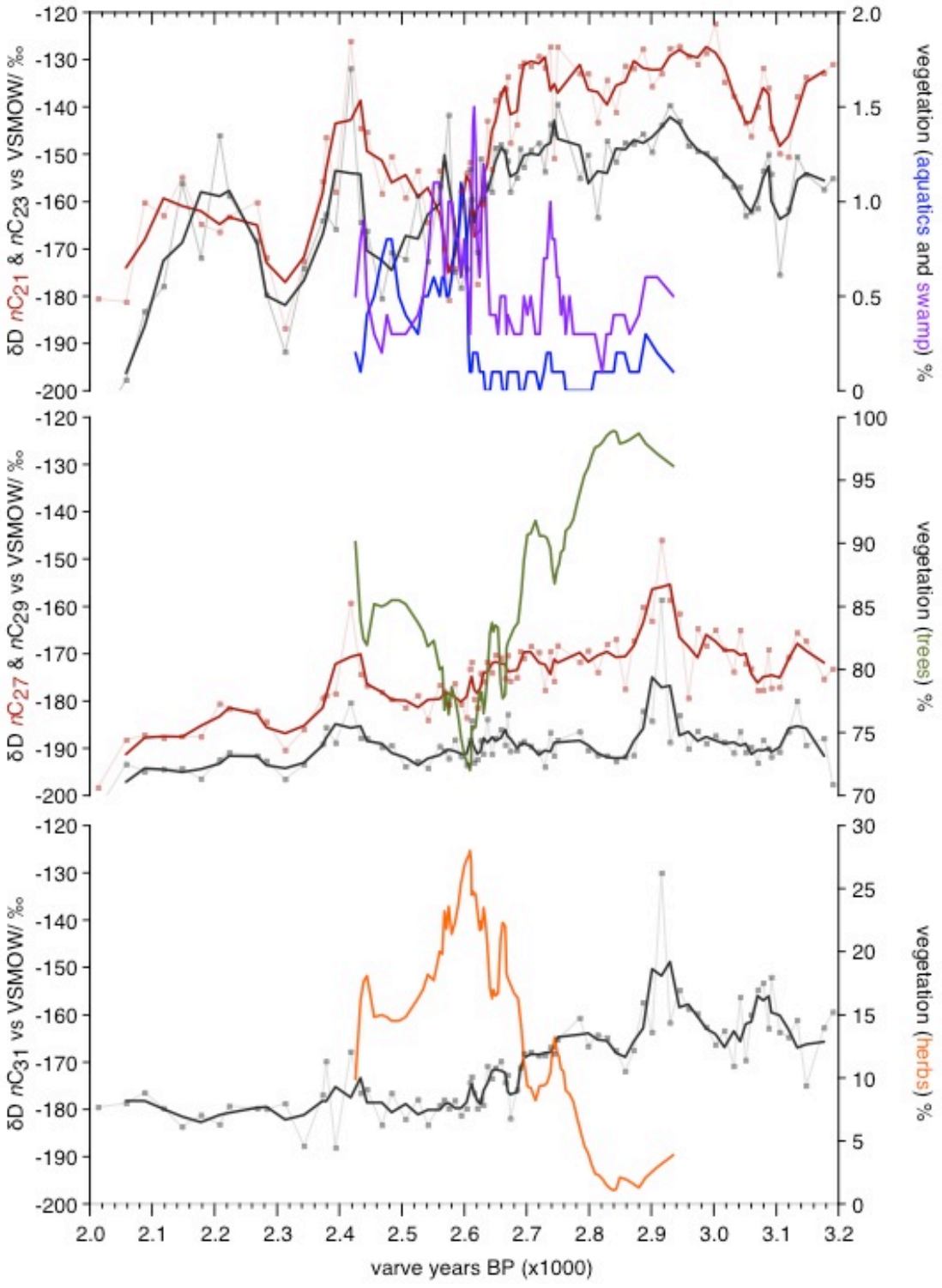

Fig. 4: Aquatic and terrestrial plant derived sedimentary *n*-alkane δD record combined with reconstructed vegetation distribution. Vegetation data shown as moving average over 3 data points. **(A)** Aquatic plant derived *n*-alkane δD records (nC_{21}, nC_{23}) vs. vegetation population of aquatic and swamp taxa. **(B)** Terrestrial plant (tree) derived *n*-alkane δD records (nC_{27}, nC_{29}) vs. tree

703 population. **(C)** Terrestrial plant (herbs) derived *n*-alkane δD record (nC$_{31}$) vs.
704 herb population.
705
706 **7. Conclusions**
707 Our combined high-resolution hydroclimate and vegetation study based on
708 lipid biomarker δD and palynological records from lake MFM provides detailed
709 insights into the succession of climate and ecosystem change and
710 emphasizes the advantages of a multiproxy approach for hydroclimate
711 reconstructions during periods of ecological change. Specifically, our results
712 indicate that:
713 (1) Between 3200 and 2000 varve years BP decreasing lipid biomarker δD
714 values reflect the overall late Holocene trend to cooler and/ or wetter
715 conditions.
716 (2) Since lipid biomarker δD values remain more negative after the HCO,
717 we suggest that this period does not only constitute a temporal climatic
718 oscillation triggered by a grand solar minimum, but marks a transition
719 phase resulting in the permanent establishment of cooler and wetter
720 conditions and/or different atmospheric moisture pathways.
721 (3) Our data show that the local aquatic ecosystem composition did
722 change significantly at 2640 varve years BP, ca. 60 years after the
723 onset of changes in the terrestrial ecosystem. This is possibly induced
724 by increased nutrient input due to enhanced soil erosion, which in turn
725 was related to a decrease in vegetation caused by forest clearance.
726 (4) We argue that changes in the source organisms of aquatic *n*-alkanes
727 (possibly associated with different degrees of biosynthetic hydrogen
728 isotope fractionation) at the time of major (aquatic) ecosystem change
729 caused significant changes in δD_{aq} values. Therefore, the appearance
730 and/or disappearance of a single species can result in significant
731 variations in sedimentary δD_{aq}, in particular for lake systems with a
732 limited number of aquatic *n*-alkane source organisms. However, while
733 *n*-alkane spectra of species-poor assemblages might be more
734 susceptible to taxonomic turnover, even changes in species-rich

assemblages could significantly affect the *n*-alkane record. As such, changes in the aquatic lipid biomarker δD values during the study period do not only reflect hydroclimate changes but also reflect ecological change, in our case amplifying the climatic signal.

(5) In contrast, terrestrial higher plant derived leaf wax *n*-alkanes, produced by a number of different broadleaved tree species and derived from thousands of individual trees in the lake catchment, record an integrated signal of the terrestrial vegetation and, therefore a more reliable hydroclimate record.

Our data suggest the importance to consider the different integrative capacities of source specific vs. less specific lipid biomarkers and show that the combination with microfossil records can provide detailed insights into the succession of climatic and ecosystem changes in the lake catchment.

Acknowledgements

This work was supported by a DFG Emmy-Noether grant to DS (SA1889/1-1). It is a contribution to the INTIMATE project, which is funded as an EU COST Action and to the Helmholtz Association (HGF) Climate Initiative “REKLIM” Topic 8 ‘Rapid climate change derived from proxy data’ and has used infrastructure of the HGF TERENO programme. Laboratory assistance was provided by Nikolas Werner (UP).

Author contributions

O. Rach carried out the *n*-alkane extraction, analysis, stable isotope measurement, isotope data evaluation and wrote the paper. S. Engels and B. van Geel carried out the pollen analysis, pollen data evaluation and wrote the paper. A. Kahmen provided infrastructure for isotope measurement, contributed to the analysis, data evaluation and writing. A. Brauer was responsible for lake coring, data evaluation and writing. C. Martín-Puertas provided the chronology and stratigraphy, contributed to data evaluation and

wrote the paper. Dirk Sachse conceived the research, acquired financial support and wrote the paper.

Supplementary information

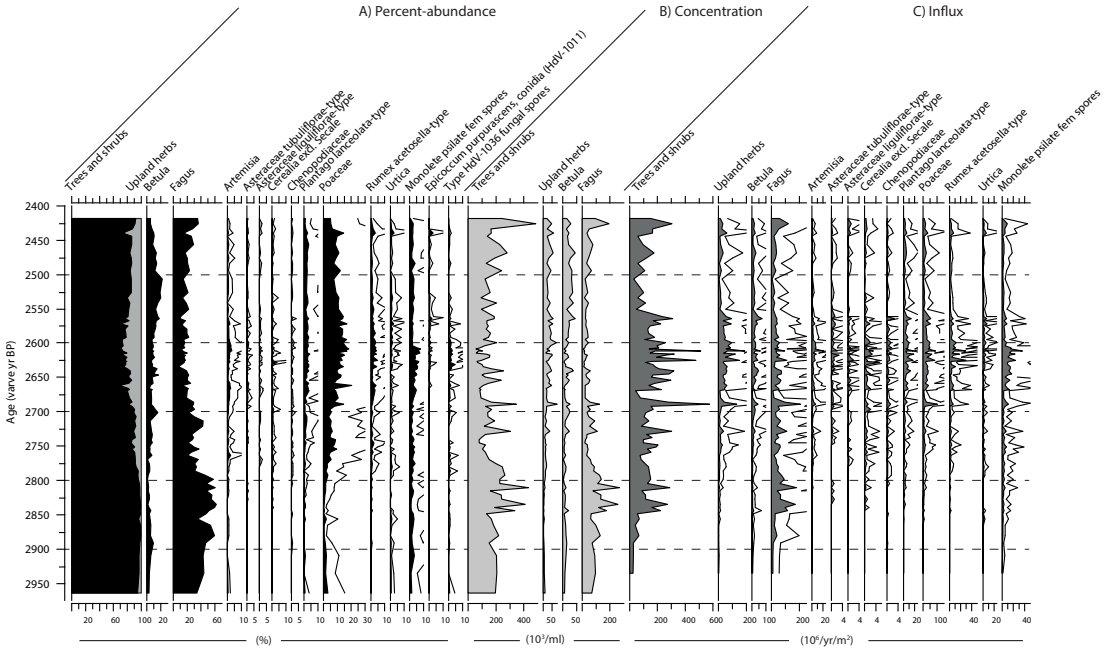

Fig. S1: Overview diagram on arboreal taxa (in percent - left, concentration – middle, influx - right)

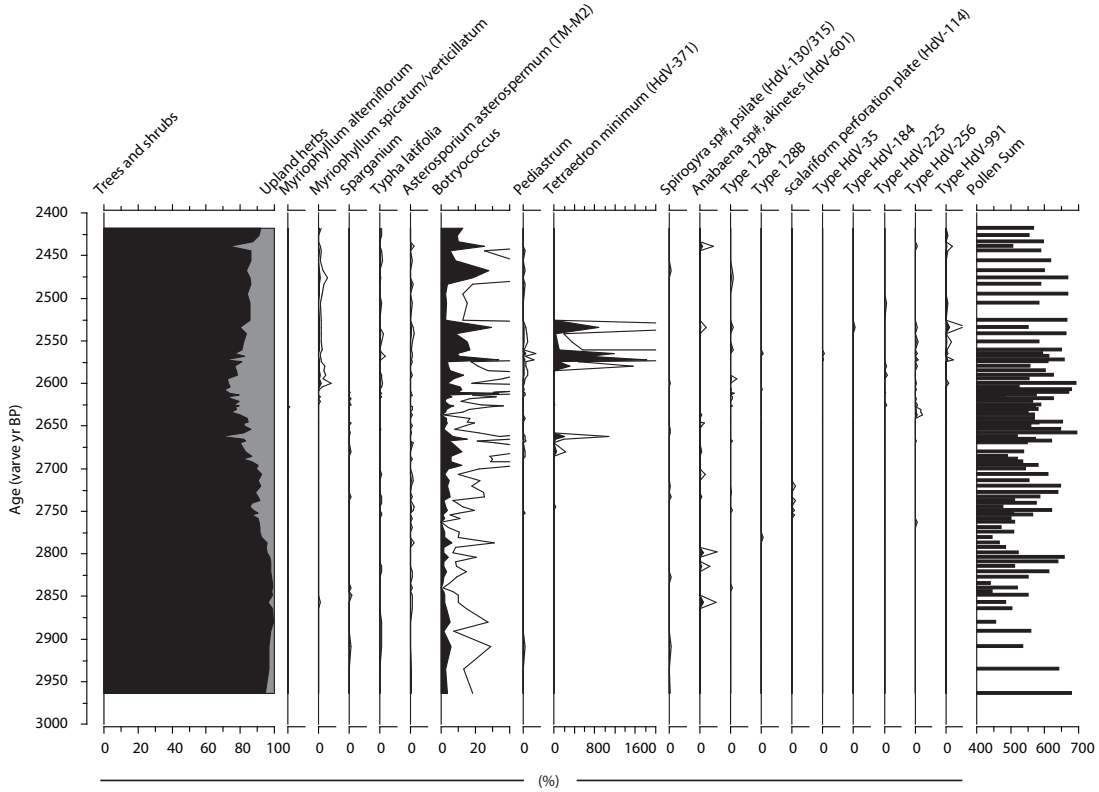

Fig. S2: Overview diagram on aquatic taxa (right part) and trees/ shrubs vs. herbaceous taxa distribution (left) in percent

References

Aichner, B., Herzschuh, U., Wilkes, H., Vieth, A., Böhner, J., 2010. δD values of n-alkanes in Tibetan lake sediments and aquatic macrophytes - A surface sediment study and application to a 16 ka record from Lake Koucha. Organic Geochemistry 41, 779-790.

Atwood, A.R., Sachs, J.P., 2014. Separating ITCZ- and ENSO-related rainfall changes in the Galápagos over the last 3 kyr using D/H ratios of multiple lipid biomarkers. Earth and Planetary Science Letters 404, 408-419.

Baas, M., Pancost, R., van Geel, B., Sinninghe Damsté, J.S., 2000. A comparative study of lipids in *Sphagnum* species. Organic Geochemistry 31, 535-541.

Baldini, L.M., McDermott, F., Foley, A.M., Baldini, J.U.L., 2008. Spatial variability in the European winter precipitation δ18O-NAO relationship: Implications for reconstructing NAO-mode climate variability in the Holocene. Geophysical Research Letters 35, L04709.

797 Behre, K.-E., 1981. The interpretation of anthropogenic indicators in pollen
798 diagrams. Pollen et spores 23, 225-245.

799 Beug, H.J., 2004. Leitfaden der Pollenbestimmung für Mitteleuropa und
800 angrenzende Gebiete. Verlag Dr. Friedrich Pfeil.

801 Brauer, A., Endres, C., Günter, C., Litt, T., Stebich, M., Negendank, J.F.W., 1999a.
802 High resolution sediment and vegetation responses to Younger Dryas climate
803 change in varved lake sediments from Meerfelder Maar, Germany. Quaternary
804 Science Reviews 18, 321-329.

805 Brauer, A., Endres, C., Negendank, J.F.W., 1999b. Lateglacial calendar year
806 chronology based on annually laminated sediments from Lake Meerfelder Maar,
807 Germany. Quaternary International 61, 17-25.

808 Brauer, A., Endres, C., Zolitschka, B., Negendank, J.F.W., 2000. AMS Radiocarbin
809 and varve chronology from the annually laminated sediment record of lake
810 Meerfelder Maar, Germany. Radiocarbon 42, 355-368.

811 Brauer, A., Haug, G.H., Dulski, P., Sigman, D.M., Negendank, J.F.W., 2008. An
812 abrupt wind shift in western Europe at the onset of the Younger Dryas cold
813 period. Nature Geoscience 1, 520-523.

814 Craig, G.L., 1965. Deuterium and oxygen 18 variations in the ocean and the
815 marine atmosphere, in: Tongiori, E. (Ed.), Stable Isotopes in Oceanographic
816 Studies and Paleotemperatures. CNR Lab. Geol. Nucl., Pisa, pp. 9–130.

817 Cranwell, P.A., Eglinton, G., Robinson, N., 1987. Lipids of aquatic organisms as
818 potential contributors to lacustrine sediments-II. Organic Geochemistry 11, 513-
819 527.

820 Dansgaard, W., 1964. Stable isotopes in precipitation. Tellus 16, 436-468.

821 Diefendorf, A.F., Freeman, K.H., Wing, S.L., Graham, H.V., 2011. Production of n-
822 alkyl lipids in living plants and implications for the geologic past. Geochimica et
823 Cosmochimica Acta 75, 7472-7485.

824 Duan, Y., He, J.X., 2011. Distribution and isotopic composition of n-alkanes from
825 grass, reed and tree leaves along a latitudinal gradient in China. Geochemical
826 Journal 45, 199-207.

827 Eglinton, G., Hamilton, R.J., 1967. Leaf epicuticular waxes. Science 156, 1322-
828 1327.

829 Eglinton, T.I., Eglinton, G., 2008. Molecular proxies for paleoclimatology. Earth
830 and Planetary Science Letters 275, 1-16.

831 Engels, S., Bakker, M., Bohncke, S., Cerli, C., Hoek, W., Jansen, B., Peters, T.,
832 Renssen, H., Sachse, D., Aken, J.v., Bos, V.v.d., Geel, B.v., Oostrom, R.v., Winkels, T.,
833 Wolma, M., 2016a. Centennial-scale lake-level lowstand at Lake Uddelermeer
834 (The Netherlands) indicates changes in moisture source region prior to the 2.8-
835 kyr event. The Holocene 26, 1075-1091.

836 Engels, S., Brauer, A., Buddelmeijer, N., Martín-Puertas, C., Rach, O., Sachse, D.,
837 van Geel, B., 2016b. Subdecadal-scale vegetation responses to a previously
838 unknown late-Allerød climate fluctuation and Younger Dryas cooling at Lake
839 Meerfelder Maar (Germany). Journal of Quaternary Science 31, 741-752.

840 Faegri, K., Iversen, J., Kaland, P.E., Krzywinski, K., 1990. Textbook of pollen
841 analysis, 4 ed. John Wiley & Sons, Ltd, Chichester.

842 Farquhar, G.D., Cernusak, L.A., Barnes, B., 2007. Heavy water fractionation during
843 transpiration. Plant Physiol. 143, 11-18.

844 Feakins, S.J., Kirby, M.E., Cheetham, M.I., Ibarra, Y., Zimmerman, S.R.H., 2014.
845 Fluctuation in leaf wax D/H ratio from a southern California lake records
846 significant variability in isotopes in precipitation during the late Holocene.
847 Organic Geochemistry 66, 48-59.

848 Ficken, K.J., Li, B., Swain, D.L., Eglinton, G., 2000. An n-alkane proxy for the
849 sedimentary input of submerged/floating freshwater aquatic macrophytes.
850 Organic Geochemistry 31, 745-749.

851 Flanagan, L.B., Comstock, J.P., Ehleringer, J.R., 1991. Comparison of modeled and
852 observed environmental influences on the stable oxygen and hydrogen isotope
853 composition of leaf water in *Phaseolus vulgaris*. Plant Physiol. 96, 588-596.

854 Gao, L., Edwards, E.J., Zeng, Y.B., Huang, Y.S., 2014. Major Evolutionary Trends in
855 Hydrogen Isotope Fractionation of Vascular Plant Leaf Waxes. Plos One 9.

856 Gao, L., Hou, J., Toney, J., MacDonald, D., Huang, Y., 2011. Mathematical modeling
857 of the aquatic macrophyte inputs of mid-chain n-alkyl lipids to lake sediments:
858 Implications for interpreting compound specific hydrogen isotopic records.
859 Geochimica et Cosmochimica Acta 75, 3781-3791.

860 Garcin, Y., Schwab, V.F., Gleixner, G., Kahmen, A., Todou, G., Sene, O., Onana, J.M.,
861 Achoundong, G., Sachse, D., 2012. Hydrogen isotope ratios of lacustrine
862 sedimentary n-alkanes as proxies of tropical African hydrology: Insights from a
863 calibration transect across Cameroon. Geochimica et Cosmochimica Acta 79,
864 106-126.

865 Gat, J.R., 1996. Oxygen and Hydrogen isotopes in the hydrologic cycle. Annual
866 Review of Earth and Planetary Sciences 24, 225-262.

867 Gat, J.R., Mook, W.G., Meijer, H.A.J., 2000. Environmental Isotopes in
868 the Hydrological Cycle - Principles and Applications - Volume 2: Atmospheric
869 Water, Atmospheric Water. International Atomic Energy Agency and United
870 Nations Educational, Scientific and Cultural Organization, Paris Vienna.

871 Gelpi, E., Schneider, H., Mann, J., Oro, J., 1970. Hydrocarbons of geochemical
872 significance in microscopic algae. Phytochemistry 9, 603-612.

873 Hou, J., D'Andrea, W.J., MacDonald, D., Huang, Y., 2007. Hydrogen isotopic
874 variability in leaf waxes among terrestrial and aquatic plants around Blood Pond,
875 Massachusetts (USA). Organic Geochemistry 38, 977-984.

876 Huang, Y., Shuman, B., Wang, Y., Webb, T., 2004. Hydrogen isotope ratios of
877 individual lipids in lake sediments as novel tracers of climatic and environmental
878 change: a surface sediment test. Journal of Paleolimnology 31, 363-375.

879 IAEA/WMO, 2006. Global Network of Isotopes in Precipitation. The GNIP
880 Database, Bundesanstalt fuer Gewaesserkunde.

881 Kahmen, A., Hoffmann, B., Schefuss, E., Arndt, S.K., Cernusak, L.A., West, J.B.,
882 Sachse, D., 2013a. Leaf water deuterium enrichment shapes leaf wax n-alkane
883 delta D values of angiosperm plants II: Observational evidence and global
884 implications. Geochimica et Cosmochimica Acta 111, 50-63.

885 Kahmen, A., Sachse, D., Arndt, S.K., Tu, K.P., Farrington, H., Vitousek, P.M.,
886 Dawson, T.E., 2011. Cellulose delta(18)O is an index of leaf-to-air vapor pressure
887 difference (VPD) in tropical plants. Proceedings of the National Academy of
888 Sciences 108, 1981-1986.

889 Kahmen, A., Schefuss, E., Sachse, D., 2013b. Leaf water deuterium enrichment
890 shapes leaf wax n-alkane delta D values of angiosperm plants I: Experimental
891 evidence and mechanistic insights. Geochimica et Cosmochimica Acta 111, 39-49.

892 Killops, S., Killops, V., 2005. Introduction to organic geochemistry, 2nd ed.
893 Blackwell Publishing, Malden (USA), Oxford (UK), Carlton (Australia).

894 Kubitz, B., 2000. History of Holocene vegetation and human settlement in
895 Western Eifel (Germany) based on a high-resolution pollen diagram from the
896 Meerfelder Maar Lake, [Dissertationes Botanicae. History of Holocene vegetation
897 and human settlement in Western Eifel. J. Cramer in der Gebrueder Borntraeger
898 Verlagsbuchhandlung , D-14129, Berlin, Germany, pp. 1-106.

899 Landolt, E., Bäumler, B., 2010. Flora indicativa: ökologische Zeigerwerte und
900 biologische Kennzeichen zur Flora der Schweiz und der Alpen. Ed. des
901 Conservatoire et Jardin botaniques de la ville de Genève.

902 Lauber, K., Wagner, G., 2001. Flora Helvetica, 3. Auflage ed. Verlag Paul Haupt,
903 Bern; Stuttgart; Wien.

904 Litt, T., Brauer, A., Goslar, T., Merkt, J., Balaga, K., M¸ller, H., Ralska-Jasiewiczowa,
905 M., Stebich, M., Negendank, J.F.W., 2001. Correlation and synchronisation of
906 Lateglacial continental sequences in northern central Europe based on annually
907 laminated lacustrine sediments. Quaternary Science Reviews 20, 1233-1249.

908 Litt, T., Scholzel, C., Kuhl, N., Brauer, A., 2009. Vegetation and climate history in
909 the Westeifel Volcanic Field (Germany) during the past 11000 years based on
910 annually laminated lacustrine maar sediments. Boreas 38, 679-690.

911 Liu, W.G., Yang, H., Li, L.W., 2006. Hydrogen isotopic compositions of n-alkanes
912 from terrestrial plants correlate with their ecological life forms. Oecologia 150,
913 330-338.

914 Magny, M., 1993. Solar influences on Holocene climate changes illustrated by
915 correlations between past lake-level fluctuations and the atmospheric C14
916 record. Quaternary Research 40, 1-9.

917 Marcott, S.A., Shakun, J.D., Clark, P.U., Mix, A.C., 2013. A Reconstruction of
918 Regional and Global Temperature for the Past 11,300 Years. Science 339, 1198-
919 1201.

920 Martin-Puertas, C., Brauer, A., Dulski, P., Brademann, B., 2012a. Testing climate-
921 proxy stationarity throughout the Holocene: an example from the varved
922 sediments of Lake Meerfelder Maar (Germany). Quaternary Science Reviews 58,
923 56-65.

924 Martin-Puertas, C., Matthes, K., Brauer, A., Muscheler, R., Hansen, F., Petrick, C.,
925 Aldahan, A., Possnert, G., van Geel, B., 2012b. Regional atmospheric circulation
926 shifts induced by a grand solar minimum. Nature Geoscience 5, 397-401.

927 Massimo, M., 1996. Chemotaxonomic significance of leaf wax alkanes in the
928 Gramineae. Biochemical Systematics and Ecology 24, 53-64.

929 McInerney, F.A., Helliker, B.R., Freeman, K.H., 2011. Hydrogen isotope ratios of
930 leaf wax n-alkanes in grasses are insensitive to transpiration. Geochimica et
931 Cosmochimica Acta 75, 541-554.

932 Moore, P.D., Webb, J.A., Collinson, M.E., 1991. Pollen analysis, Second edition.
933 Blackwell Scientific Publications, 3 Cambridge Center, Cambridge, Massachusetts
934 02142, USA Osney Mead, Oxford OX2 0EL, England.

Moschen, R., Lucke, A., Schleser, G.H., 2005. Sensitivity of biogenic silica oxygen isotopes to changes in surface water temperature and palaeoclimatology. Geophysical Research Letters 32.

Movius, H.L., 2013. The Irish Stone Age. Cambridge University Press.

Nelson, D.M., Henderson, A.K., Huang, Y.S., Hu, F.S., 2013. Influence of terrestrial vegetation on leaf wax delta D of Holocene lake sediments. Organic Geochemistry 56, 106-110.

Parrish, C.C., 1988. Dissolved and particulate marine lipid classes - a review. Marine Chemistry 23, 17-40.

Peters, K.E., Moldowan, J.M., Walters, C.C., 2007. The Biomarker Guide: Volume 1, Biomarkers and Isotopes in the Environment and Human History. Cambridge University Press.

Piasentier, E., Bovolenta, S., Malossini, F., 2000. The n-alkane concentrations in buds and leaves of browsed broadleaf trees. Journal of Agricultural Science 135, 311-320.

Rach, O., Brauer, A., Wilkes, H., Sachse, D., 2014. Delayed hydrological response to Greenland cooling at the onset of the Younger Dryas in western Europe. Nature Geoscience 7, 109-112.

Reimer, P.J., Baillie, M.G.L., Bard, E., Bayliss, A., Beck, J.W., Blackwell, P.G., Ramsey, C.B., Buck, C.E., Burr, G.S., Edwards, R.L., Friedrich, M., Grootes, P.M., Guilderson, T.P., Hajdas, I., Heaton, T.J., Hogg, A.G., Hughen, K.A., Kaiser, K.F., Kromer, B., McCormac, F.G., Manning, S.W., Reimer, R.W., Richards, D.A., Southon, J.R., Talamo, S., Turney, C.S.M., van der Plicht, J., Weyhenmeye, C.E., 2009. Intcal09 and Marine09 radiocarbon age clibration curves, 0-50.000 years cal BP. Radiocarbon 51, 1111-1150.

Renssen, H., Seppä, H., Heiri, O., Roche, D.M., Goosse, H., Fichefet, T., 2009. The spatial and temporal complexity of the Holocene thermal maximum. Nature Geoscience 2, 410-413.

Sachs, J.P., 2014. Hydrogen Isotope Signatures in the Lipids of Phytoplankton, in: Holland, H.D., Turekian, K.K. (Eds.), Treatise on Geochemistry, Second Edition ed. Elsevier, Oxford, pp. 79-94.

Sachs, J.P., Pahnke, K., Smittenberg, R., Zhang, Z., 2013. Biomarker Indicators of Past Climate, in: Mock, S.A.E.J. (Ed.), Encyclopedia of Quaternary Science (Second Edition). Elsevier, Amsterdam, pp. 775-782.

969 Sachs, J.P., Sachse, D., Smittenberg, R.H., Zhang, Z.H., Battisti, D.S., Golubic, S.,
970 2009. Southward movement of the Pacific intertropical convergence zone AD
971 1400-1850. Nature Geoscience 2, 519-525.

972 Sachse, D., Billault, I., Bowen, G.J., Chikaraishi, Y., Dawson, T.E., Feakins, S.J.,
973 Freeman, K.H., Magill, C.R., McInerney, F.A., van der Meer, M.T.J., Polissar, P.,
974 Robins, R.J., Sachs, J.P., Schmidt, H.-L., Sessions, A.L., White, J.W.C., West, J.B.,
975 Kahmen, A., 2012. Molecular Paleohydrology: Interpreting the Hydrogen-
976 Isotopic Composition of Lipid Biomarkers from Photosynthesizing Organisms.
977 Annual Review of Earth and Planetary Sciences 40, 221-249.

978 Sachse, D., Radke, J., Gleixner, G., 2004. Hydrogen isotope ratios of recent
979 lacustrine sedimentary n-alkanes record modern climate variability. Geochimica
980 et Cosmochimica Acta 68, 4877-4889.

981 Sachse, D., Radke, J., Gleixner, G., 2006. δD values of individual n-alkanes from
982 terrestrial plants along a climatic gradient - Implications for the sedimentary
983 biomarker record. Organic Geochemistry 37, 469-483.

984 Sachse, D., Sachs, J.P., 2008. Inverse relationship between D/H fractionation in
985 cyanobacterial lipids and salinity in Christmas Island saline ponds. Geochimica et
986 Cosmochimica Acta 72, 793-806.

987 Sauer, P.E., Eglinton, T.I., Hayes, J.M., Schimmelmann, A., Sessions, A.L., 2001.
988 Compound-specific D/H ratios of lipid biomarkers from sediments as a proxy for
989 environmental and climatic conditions. Geochimica et Cosmochimica Acta 65,
990 213-222.

991 Schefuss, E., Kuhlmann, H., Mollenhauer, G., Prange, M., Pätzold, J., 2011. Forcing
992 of wet phases in southeast Africa over the past 17,000 years. Nature 480, 509-
993 512.

994 Scott, E.M., Alekseev, A.Y., Zaitseva, G., 2006. Impact of the Environment on
995 Human Migration in Eurasia: Proceedings of the NATO Advanced Research
996 Workshop, held in St. Petersburg, 15-18 November 2003. Springer Netherlands.

997 Sessions, A.L., Burgoyne, T.W., Schimmelmann, A., Hayes, J.M., 1999.
998 Fractionation of hydrogen isotopes in lipid biosynthesis. Organic Geochemistry
999 30, 1193-1200.

1000 Sessions, A.L., Hayes, J.M., 2005. Calculation of hydrogen isotopic fractionations
1001 in biogeochemical systems. Geochimica et Cosmochimica Acta 69, 593-597.

1002 Smittenberg, R.H., Saenger, C., Dawson, M.N., Sachs, J.P., 2011. Compound-specific
1003 D/H ratios of the marine lakes of Palau as proxies for West Pacific Warm Pool
1004 hydrologic variability. Quaternary Science Reviews 30, 921-933.

1005 Stockmarr, J., 1971. Tablets with spores used in absolute pollen analysis. Pollen
1006 et Spores 13, 615-621.

1007 Swierczynski, T., Lauterbach, S., Dulski, P., Delgado, J., Merz, B., Brauer, A., 2013.
1008 Mid- to late Holocene flood frequency changes in the northeastern Alps as
1009 recorded in varved sediments of Lake Mondsee (Upper Austria). Quaternary
1010 Science Reviews 80, 78-90.

1011 Tierney, J.E., Oppo, D.W., Rosenthal, Y., Russell, J.M., Linsley, B.K., 2010.
1012 Coordinated hydrological regimes in the Indo-Pacific region during the past two
1013 millennia. Paleoceanography 25.

1014 Tierney, J.E., Russell, J.M., Huang, Y.S., Sinninghe Damsté, J.S., Hopmans, E.C.,
1015 Cohen, A.S., 2008. Northern hemisphere controls on tropical southeast African
1016 climate during the past 60,000 years. Science 322, 252-255.

1017 Van Geel, B., 1978. A palaeoecological study of holocene peat bog sections in
1018 Germany and The Netherlands, based on the analysis of pollen, spores and
1019 macro- and microscopic remains of fungi, algae, cormophytes and animals.
1020 Review of Palaeobotany and Palynology 25, 1-120.

1021 van Geel, B., Berglund, B.E., 2000. A causal link between a climatic deterioration
1022 around 850 cal BC and a subsequent rise in human population density in NW-
1023 Europe? Terra Nostra 7, 126-130.

1024 van Geel, B., Buurman, J., Waterbolk, H.T., 1996. Archaeological and
1025 palaeoecological indications of an abrupt climate change in The Netherlands, and
1026 evidence for climatological teleconnections around 2650 BP. Journal of
1027 Quaternary Science 11, 451-460.

1028 van Geel, B., Engels, S., Martin-Puertas, C., Brauer, A., 2013. Ascospores of the
1029 parasitic fungus *Kretzschmaria deusta* as rainstorm indicators during a late
1030 Holocene beech-forest phase around lake Meerfelder Maar, Germany. Journal of
1031 Paleolimnology 50, 33-40.

1032 van Geel, B., Raspopov, O.M., Renssen, H., van der Plicht, J., Dergachev, V.A.,
1033 Meijer, H.A.J., 1999. The role of solar forcing upon climate change. Quaternary
1034 Science Reviews 18, 331-338.

1035 Vonmoos, M., Beer, J., Muscheler, R., 2006. Large variations in Holocene solar
1036 activity: Constraints from Be-10 in the Greenland Ice Core Project ice core.
1037 Journal of Geophysical Research-Space Physics 111.

1038 Wanner, H., Beer, J., Butikofer, J., Crowley, T.J., Cubasch, U., Fluckiger, J., Goosse,
1039 H., Grosjean, M., Joos, F., Kaplan, J.O., Kuttel, M., Muller, S.A., Prentice, I.C.,
1040 Solomina, O., Stocker, T.F., Tarasov, P., Wagner, M., Widmann, M., 2008. Mid- to

1041 Late Holocene climate change: an overview. Quaternary Science Reviews 27,
1042 1791-1828.

1043 Wirth, S.B., Glur, L., Gilli, A., Anselmetti, F.S., 2013. Holocene flood frequency
1044 across the Central Alps – solar forcing and evidence for variations in North
1045 Atlantic atmospheric circulation. Quaternary Science Reviews 80, 112-128.

1046 Zhang, Z., Leduc, G., Sachs, J.P., 2014. El Niño evolution during the Holocene
1047 revealed by a biomarker rain gauge in the Galápagos Islands. Earth and Planetary
1048 Science Letters 404, 420-434.

1049 Zhang, Z., Sachs, J.P., 2007. Hydrogen isotope fractionation in freshwater algae: I.
1050 Variations among lipids and species. Organic Geochemistry 38, 582-608.

1051 Zolitschka, B., Brauer, A., Negendank, J.F.W., Stockhausen, H., Lang, A., 2000.
1052 Annually dated late Weichselian continental paleoclimate record from the Eifel,
1053 Germany. Geology 28, 783-786.

1054 Zöller, L., Blanchard, H., 2009. The partial heat – longest plateau technique:
1055 Testing TL dating of Middle and Upper Quaternary volcanic eruptions in the Eifel
1056 Area, Germany. E&G - Quaternary Science Journal 58, p. 86-107.
1057
1058